Region Filling and Object Removal by Exemplar-Based Image Inpainting

A. Criminisi*, P. Pérez and K. Toyama
Microsoft Research, Cambridge (UK) and Redmond (US)
antcrim@microsoft.com

Abstract— **A new algorithm is proposed for removing large objects from digital images. The challenge is to fill in the hole that is left behind in a visually plausible way.**

In the past, this problem has been addressed by two classes of algorithms: (i) "texture synthesis" algorithms for generating *large* image regions from sample textures, and (ii) "inpainting" techniques for filling in *small* image gaps. The former has been demonstrated for "textures" – repeating two-dimensional patterns with some stochasticity; the latter focus on linear "structures" which can be thought of as one-dimensional patterns, such as lines and object contours.

This paper presents a novel and efficient algorithm that combines the advantages of these two approaches. We first note that exemplar-based texture synthesis contains the essential process required to replicate both texture and structure; the success of structure propagation, however, is highly dependent on the *order* in which the filling proceeds. We propose a best-first algorithm in which the *confidence* in the synthesized pixel values is propagated in a manner similar to the propagation of information in inpainting. The actual colour values are computed using exemplar-based synthesis.

In this paper the simultaneous propagation of texture and structure information is achieved by a *single*, efficient algorithm. Computational efficiency is achieved by a block-based sampling process.

A number of examples on real and synthetic images demonstrate the effectiveness of our algorithm in removing large occluding objects as well as thin scratches. Robustness with respect to the shape of the manually selected target region is also demonstrated. Our results compare favorably to those obtained by existing techniques.

Keywords— **Object Removal, Image Inpainting, Texture Synthesis, Simultaneous Texture and Structure Propagation.**

I. Introduction

This paper presents a novel algorithm for removing large objects from digital photographs and replacing them with visually plausible backgrounds. Figure 1 shows an example of this task, where the foreground person (manually selected as the *target region*) is automatically replaced by data sampled from the remainder of the image. The algorithm effectively hallucinates new colour values for the target region in a way that looks "reasonable" to the human eye. This paper builds upon and extends the work in [8], with a more detailed description of the algorithm and extensive comparisons with the state of the art.

In previous work, several researchers have considered texture synthesis as a way to fill large image regions with "pure" textures – repetitive two-dimensional textural patterns with moderate stochasticity. This is based on a large body of texture-synthesis research, which seeks to replicate texture *ad infinitum*, given a small source sample of pure texture [1], [9], [11], [12], [13], [14], [16], [17], [18], [22], [25]. Of particular interest are *exemplar-based techniques* which cheaply and effectively generate new texture by sampling and copying colour values from the source [1], [11], [12], [13], [17].

As effective as these techniques are in replicating consistent texture, they have difficulty filling holes in photographs of real-world scenes, which often consist of linear structures and *composite textures* – multiple textures interacting spatially [26]. The main problem is that boundaries between image regions are a complex product of mutual influences between different textures. In constrast to the two-dimensional nature of pure textures, these boundaries form what might be considered more one-dimensional, or linear, image structures.

a **b**

Fig. 1. **Removing large objects from images.** (a) Original photograph. (b) The region corresponding to the foreground person (covering about 19% of the image) has been manually selected and then automatically removed. Notice that the horizontal structures of the fountain have been synthesized in the occluded area together with the water, grass and rock textures.

A number of algorithms specifically address the image filling issue for the task of image restoration, where speckles, scratches, and overlaid text are removed [2], [3], [4], [7], [23]. These *image inpainting* techniques fill holes in images by propagating linear structures (called *isophotes* in the inpainting literature) into the target region via diffusion. They are inspired by the partial differential equations of physical heat flow, and work convincingly as restoration algorithms. Their drawback is that the diffusion process introduces some blur, which becomes noticeable when filling larger regions.

The technique presented here combines the strengths of both approaches into a single, efficient algorithm. As with inpainting, we pay special attention to linear structures. But, linear structures abutting the target region only influence the fill order of what is at core an exemplar-based texture synthesis algorithm. The result is an algorithm that has the efficiency and qualitative performance of exemplar-based texture synthesis, but which also respects the image constraints imposed by surrounding linear structures.

The algorithm we propose in this paper builds on very recent research along similar lines. The work in [5] decomposes the original image into two components; one of which is processed

by inpainting and the other by texture synthesis. The output image is the sum of the two processed components. This approach still remains limited to the removal of small image gaps, however, as the diffusion process continues to blur the filled region (*cf*. [5], fig.5 top right). The automatic switching between "pure texture-" and "pure structure-mode" of [24] is also avoided.

Similar to [5] is the work in [10], where the authors describe an algorithm that interleaves a smooth approximation with example-based detail synthesis for image completion. Like the work in [5] also the algorithm in [10] is extremely slow (as reported processing may take between 83 and 158 minutes on a 384×256 image) and it may introduce blur artefacts (*cf*. fig.8b, last row of fig.13 and fig. 16c in [10]). In this paper we present a simpler and faster region filling algorithm which does not suffer from blur artefacts.

One of the first attempts to use exemplar-based synthesis specifically for object removal was by Harrison [15]. There, the order in which a pixel in the target region is filled was dictated by the level of "texturedness" of the pixel's neighborhood[1]. Although the intuition is sound, strong linear structures were often overruled by nearby noise, minimizing the value of the extra computation. A related technique drove the fill order by the local shape of the target region, but did not seek to explicitly propagate linear structures [6].

Recently Jia *et al*. [19] have presented a technique for filling image regions based on a texture-segmentation step and a tensor-voting algorithm for the smooth linking of structures across holes. Their approach has a clear advantage in that it is designed to connect curved structures by the explicit generation of subjective contours, over which textural structures are propagated. On the other hand, their algorithm requires (i) an expensive segmentation step, and (ii) a hard decision about what constitutes a boundary between two textures. Our approach avoids both issues through the use of a continuous parameter based on local gradient strength only. A careful fusion of these approaches may result in a superior algorithm, but results suggest that both approaches already achieve a reasonable measure of visual credibility in filling holes.

Finally, Zalesny *et al*. [26] describe an algorithm for the parallel synthesis of composite textures. They devise a special-purpose solution for synthesizing the interface between two "knitted" textures. In this paper we show that, in fact, only one mechanism is sufficient for the synthesis of both pure and composite textures.

Paper outline. Section II presents the two key observations which form the basis of our algorithm. The details of the proposed algorithm are described in sect. III. Finally, a large gallery of results on both synthetic images and real-scene photographs is presented in sect. IV. Whenever possible our results are compared to those obtained by state of the art techniques.

II. Key observations

A. Exemplar-based synthesis suffices

The core of our algorithm is an isophote-driven image-sampling process. It is well-understood that exemplar-based approaches perform well for two-dimensional textures [1], [11], [17]. But, we note in addition that exemplar-based texture synthesis is sufficient for propagating extended linear image structures, as well; *i.e*., a separate synthesis mechanism is not required for handling isophotes.

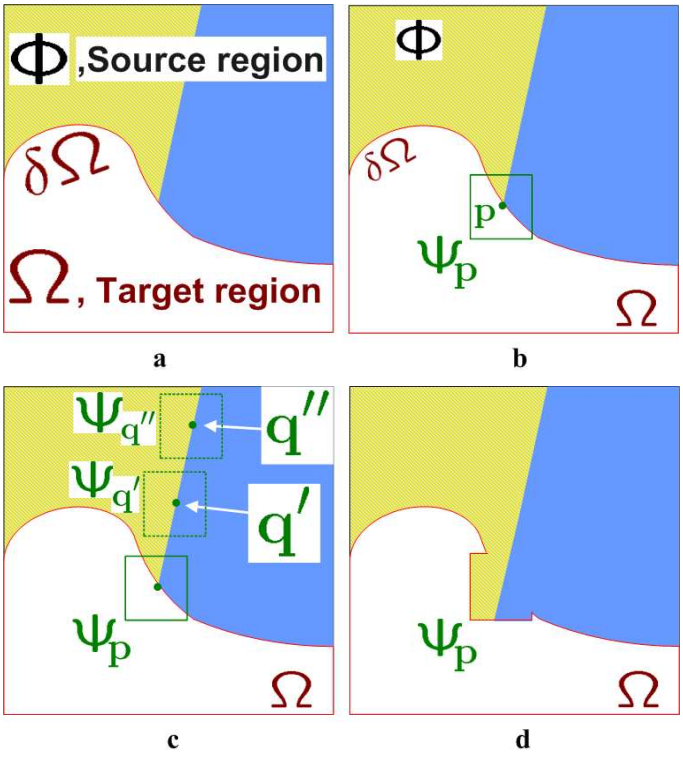

Fig. 2. **Structure propagation by exemplar-based texture synthesis.** (a) Original image, with the *target region* Ω, its contour $\delta\Omega$, and the *source region* Φ clearly marked. (b) We want to synthesize the area delimited by the patch $\Psi_{\mathbf{p}}$ centred on the point $\mathbf{p} \in \delta\Omega$. (c) The most likely candidate matches for $\Psi_{\mathbf{p}}$ lie along the boundary between the two textures in the source region, *e.g*., $\Psi_{\mathbf{q}'}$ and $\Psi_{\mathbf{q}''}$. (d) The best matching patch in the candidates set has been copied into the position occupied by $\Psi_{\mathbf{p}}$, thus achieving partial filling of Ω. Notice that both texture and structure (the separating line) have been propagated inside the target region. The target region Ω has, now, shrank and its front $\delta\Omega$ has assumed a different shape.

Figure 2 illustrates this point. For ease of comparison, we adopt notation similar to that used in the inpainting literature. The region to be filled, *i.e*., the *target* region is indicated by Ω, and its contour is denoted $\delta\Omega$. The contour evolves inward as the algorithm progresses, and so we also refer to it as the "fill front". The *source* region, Φ, which remains fixed throughout the algorithm, provides samples used in the filling process.

We now focus on a single iteration of the algorithm to show how structure and texture are adequately handled by exemplar-based synthesis. Suppose that the square template $\Psi_{\mathbf{p}} \in \Omega$ centred at the point $\mathbf{p}$ (fig. 2b), is to be filled. The best-match sample from the source region comes from the patch $\Psi_{\hat{\mathbf{q}}} \in \Phi$, which is most similar to those parts that are already filled in $\Psi_{\mathbf{p}}$. In the example in fig. 2b, we see that if $\Psi_{\mathbf{p}}$ lies on the continuation of an image edge, the most likely best matches will lie along the same (or a similarly coloured) edge (*e.g*., $\Psi_{\mathbf{q}'}$ and $\Psi_{\mathbf{q}''}$ in fig. 2c).

All that is required to propagate the isophote inwards is a simple transfer of the pattern from the best-match source patch

[1]An implementation of Harrison's algorithm is available from `www.csse.monash.edu.au/~pfh/resynthesizer/`

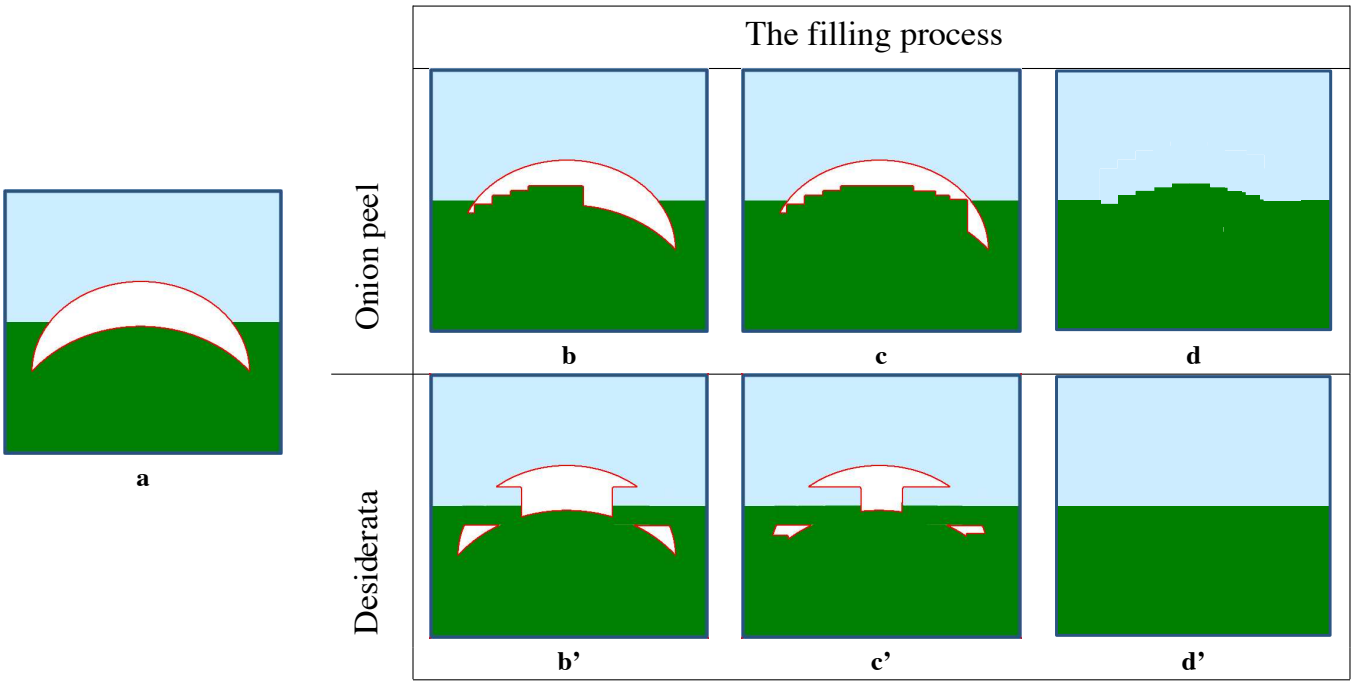

Fig. 3. **The importance of the filling order when dealing with concave target regions.** (a) A diagram showing an image and a selected target region (in white). The remainder of the image is the source. (b,c,d) Different stages in the concentric-layer filling of the target region. (d) The onion-peel approach produces artefacts in the synthesized horizontal structure. (b',c',d') Filling the target region by an edge-driven filling order achieves the desired artefact-free reconstruction. (d') The final edge-driven reconstruction, where the boundary between the two background image regions has been reconstructed correctly.

(fig. 2d). Notice that isophote orientation is automatically preserved. In the figure, despite the fact that the original edge is not orthogonal to the target contour $\delta\Omega$, the propagated structure has maintained the same orientation as in the source region.

In this work we focus on a patch-based filling approach (as opposed to pixel-based ones as in [11]) because, as noted in [22], this improves execution speed. Furthermore, we note that patch-based filling improves the accuracy of the propagated structures.

B. Filling order is critical

The previous section has shown how careful exemplar-based filling may be capable of propagating both texture and structure information. This section demonstrates that the quality of the output image synthesis is highly influenced by the order in which the filling process proceeds. Furthermore, we list a number of desired properties of the "ideal" filling algorithm.

A comparison between the standard concentric layer filling (onion-peel) and the desired filling behaviour is illustrated in fig. 3. Figures 3b,c,d show the progressive filling of a *concave* target region via an anti-clockwise onion-peel strategy. As it can be observed, this ordering of the filled patches produces the horizontal boundary between the background image regions to be unexpectedly reconstructed as a curve.

A better filling algorithm would be one that gives higher priority of synthesis to those regions of the target area which lie on the continuation of image structures, as shown in figs. 3b',c',d'. Together with the property of correct propagation of linear structures, the latter algorithm would also be more robust towards variations in the shape of the target regions.

A concentric-layer ordering, coupled with a patch-based filling may produce further artefacts (*cf.* fig. 4).

Therefore, filling order is crucial to non-parametric texture synthesis [1], [6], [12], [15]. To our knowledge, however, designing a fill order which explicitly encourages propagation of linear structure (together with texture) has never been explored, and thus far, the default favourite has been the "onion peel" strategy.

Another desired property of a good filling algorithm is that of avoiding "over-shooting" artefacts that occur when image edges are allowed to grow indefinitely. The goal here is finding a good balance between the propagation of structured regions and that of textured regions (fig. 3b',c',d'), without employing two ad-hoc strategies. As demonstrated in the next section, the algorithm we propose achieves such a balance by combining the structure "push" with a confidence term that tends to reduce sharp in-shooting appendices in the contour of the target region.

As it will be demonstrated, the filling algorithm proposed in this paper overcomes the issues that characterize the traditional concentric-layers filling approach and achieves the desired properties of: (i) correct propagation of linear structures, (ii) robustness to changes in shape of the target region, (iii) balanced simultaneous structure and texture propagation, all in a single, efficient algorithm. We now proceed with the details of our algorithm.

III. Our region-filling algorithm

First, given an input image, the user selects a target region, Ω, to be removed and filled. The source region, Φ, may be defined as the entire image minus the target region ($\Phi = \mathcal{I} - \Omega$), as a dilated band around the target region, or it may be manually specified by the user.

Next, as with all exemplar-based texture synthesis [12], the

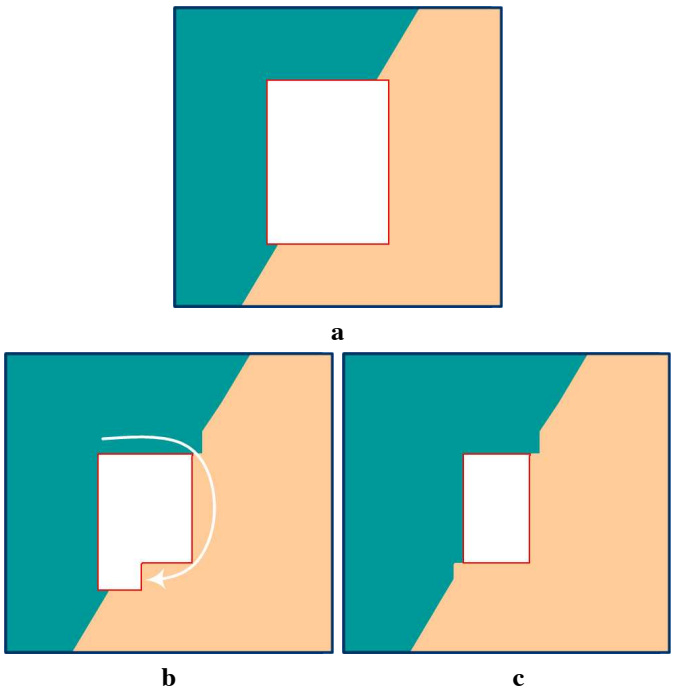

Fig. 4. **The importance of the filling order in patch-based filling.** (a) The target region is shown in white. (b) Part of the outmost layer in the target region has been synthesized by an onion-peel algorithm proceeding in clock-wise order. (c) At a further stage of the filling process, the remainder of the outmost layer has been filled by this clock-wise onion-peel filling. The concentric-layer filling has produced artefacts in the reconstruction of the diagonal image edge. A filling algorithm whose priority is guided by the image edges would fix this problem.

size of the template window Ψ must be specified. We provide a default window size of 9×9 pixels, but in practice require the user to set it to be slightly larger than the largest distinguishable texture element, or "texel", in the source region.

Once these parameters are determined, the region-filling proceeds automatically.

In our algorithm, each pixel maintains a *colour* value (or "empty", if the pixel is unfilled) and a *confidence* value, which reflects our confidence in the pixel value, and which is frozen once a pixel has been filled. During the course of the algorithm, patches along the fill front are also given a temporary *priority* value, which determines the order in which they are filled. Then, our algorithm iterates the following three steps until all pixels have been filled:

1. Computing patch priorities. Our algorithm performs the synthesis task through a best-first filling strategy that depends entirely on the priority values that are assigned to each patch on the fill front. The priority computation is biased toward those patches which: (i) are on the continuation of strong edges and (ii) are surrounded by high-confidence pixels.

Given a patch $\Psi_{\mathbf{p}}$ centred at the point $\mathbf{p}$ for some $\mathbf{p} \in \delta\Omega$ (see fig. 5), we define its priority $P(\mathbf{p})$ as the product of two terms:

$$P(\mathbf{p}) = C(\mathbf{p})D(\mathbf{p}). \tag{1}$$

We call $C(\mathbf{p})$ the *confidence* term and $D(\mathbf{p})$ the *data* term, and

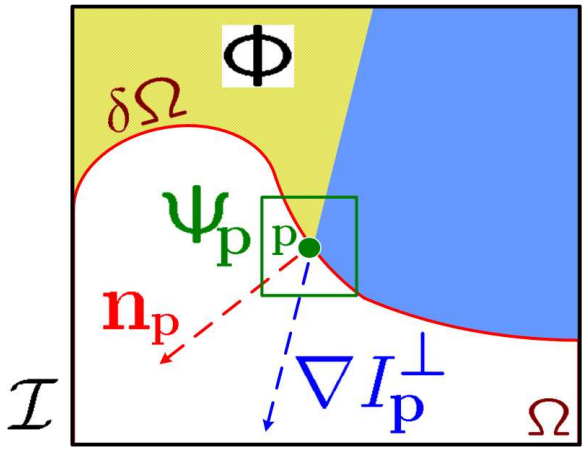

Fig. 5. **Notation diagram.** Given the patch $\Psi_{\mathbf{p}}$, $\mathbf{n}_{\mathbf{p}}$ is the normal to the contour $\delta\Omega$ of the target region Ω and $\nabla I^{\perp}_{\mathbf{p}}$ is the isophote (direction and intensity) at point $\mathbf{p}$. The entire image is denoted with $\mathcal{I}$.

they are defined as follows:

$$C(\mathbf{p}) = \frac{\sum_{\mathbf{q} \in \Psi_{\mathbf{p}} \cap (\mathcal{I} - \Omega)} C(\mathbf{q})}{|\Psi_{\mathbf{p}}|}, \qquad D(\mathbf{p}) = \frac{|\nabla I^{\perp}_{\mathbf{p}} \cdot \mathbf{n}_{\mathbf{p}}|}{\alpha}$$

where $|\Psi_{\mathbf{p}}|$ is the area of $\Psi_{\mathbf{p}}$, α is a normalization factor (*e.g.*, $\alpha = 255$ for a typical grey-level image), $\mathbf{n}_{\mathbf{p}}$ is a unit vector orthogonal to the front $\delta\Omega$ in the point $\mathbf{p}$ and $\perp$ denotes the orthogonal operator. The priority $P(\mathbf{p})$ is computed for every border patch, with distinct patches for each pixel on the boundary of the target region.

During initialization, the function $C(\mathbf{p})$ is set to $C(\mathbf{p}) = 0$ $\forall \mathbf{p} \in \Omega$, and $C(\mathbf{p}) = 1 \ \ \forall \mathbf{p} \in \mathcal{I} - \Omega$.

The confidence term $C(\mathbf{p})$ may be thought of as a measure of the amount of reliable information surrounding the pixel $\mathbf{p}$. The intention is to fill first those patches which have more of their pixels already filled, with additional preference given to pixels that were filled early on (or that were never part of the target region).

As it will be illustrated in fig. 6a, this automatically incorporates preference towards certain shapes of the fill front. For example, patches that include corners and thin tendrils of the target region will tend to be filled first, as they are surrounded by more pixels from the original image. These patches provide more reliable information against which to match. Conversely, patches at the tip of "peninsulas" of filled pixels jutting into the target region will tend to be set aside until more of the surrounding pixels are filled in.

At a coarse level, the term $C(\mathbf{p})$ of (1) approximately enforces the desirable concentric fill order. As filling proceeds, pixels in the outer layers of the target region will tend to be characterized by greater confidence values, and therefore be filled earlier; pixels in the centre of the target region will have lesser confidence values.

The data term $D(\mathbf{p})$ is a function of the strength of isophotes hitting the front $\delta\Omega$ at each iteration. This term boosts the priority of a patch that an isophote "flows" into. This factor is of fundamental importance in our algorithm because it encourages linear structures to be synthesized first, and, therefore propagated securely into the target region. Broken lines tend to con-

nect, thus realizing the "Connectivity Principle" of vision psychology [7], [20] (*cf.* fig. 7, fig. 11f', fig. 13b and fig. 20f').

2. Propagating texture and structure information. Once all priorities on the fill front have been computed, the patch $\Psi_{\hat{\mathbf{p}}}$ with highest priority is found. We then fill it with data extracted from the source region Φ.

In traditional inpainting techniques, pixel-value information is propagated via diffusion. As noted previously, diffusion necessarily leads to image smoothing, which results in blurry fill-in, especially of large regions (see fig. 15f).

On the contrary, we propagate image texture by direct sampling of the source region. Similar to [12], we search in the source region for that patch which is most similar to $\Psi_{\hat{\mathbf{p}}}$.[2] Formally,

$$\Psi_{\hat{\mathbf{q}}} = \arg\min_{\Psi_{\mathbf{q}} \in \Phi} d(\Psi_{\hat{\mathbf{p}}}, \Psi_{\mathbf{q}}) \qquad (2)$$

where the distance $d(\Psi_{\mathbf{a}}, \Psi_{\mathbf{b}})$ between two generic patches $\Psi_{\mathbf{a}}$ and $\Psi_{\mathbf{b}}$ is simply defined as the sum of squared differences (SSD) of the already filled pixels in the two patches. Pixel colours are represented in the `CIE Lab` colour space [21] because of its property of perceptual uniformity[3].

Having found the source *exemplar* $\Psi_{\hat{\mathbf{q}}}$, the value of each pixel-to-be-filled, $\mathbf{p}' \quad |\mathbf{p}' \in \Psi_{\hat{\mathbf{p}} \cap \Omega}$, is copied from its corresponding position inside $\Psi_{\hat{\mathbf{q}}}$.

This suffices to achieve the propagation of both structure and texture information from the source Φ to the target region Ω, one patch at a time (*cf.*, fig. 2d). In fact, we note that any further manipulation of the pixel values (*e.g.*, adding noise, smoothing etc.) that does not explicitly depend upon statistics of the source region, is more likely to degrade visual similarity between the filled region and the source region, than to improve it.

3. Updating confidence values. After the patch $\Psi_{\hat{\mathbf{p}}}$ has been filled with new pixel values, the confidence $C(\mathbf{p})$ is updated in the area delimited by $\Psi_{\hat{\mathbf{p}}}$ as follows:

$$C(\mathbf{p}) = C(\hat{\mathbf{p}}) \quad \forall \mathbf{p} \in \Psi_{\hat{\mathbf{p}}} \cap \Omega.$$

This simple update rule allows us to measure the relative confidence of patches on the fill front, without image-specific parameters. As filling proceeds, confidence values decay, indicating that we are less sure of the colour values of pixels near the centre of the target region.

A pseudo-code description of the algorithmic steps is shown in table I. The superscript t indicates the current iteration.

Some properties of our region-filling algorithm. As illustrated in fig. 6a, the effect of the confidence term is that of smoothing the contour of the target region by removing sharp appendices and making the target contour close to circular. Also, in fig. 6a it can be noticed that inwards-pointing appendices are discouraged by the confidence term (red corresponds to low priority pixels).

Unlike previous approaches, the presence of the data term in the priority function (1) tends to favour inwards-growing appendices in the places where structures hit the contour (green pixels in fig. 6b), thus achieving the desired structure propagation.

[2] Valid patches must be entirely contained in Φ.

[3] Euclidean distances in Lab colour space are more meaningful than in RGB space.

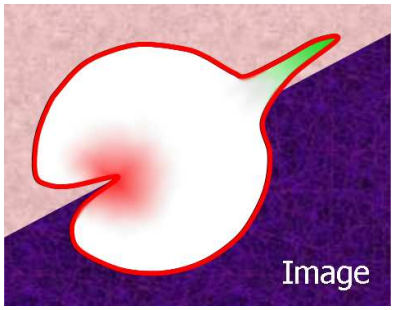

a

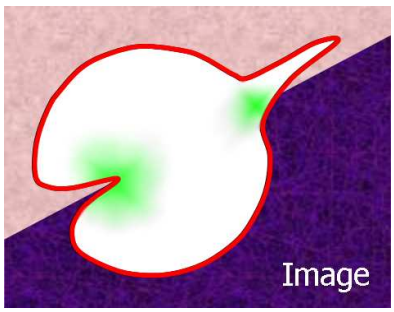

b

Fig. 6. **Effects of data and confidence terms.** (a) The *confidence term* assigns high filling priority to out-pointing appendices (in green) and low priority to in-pointing ones (in red), thus trying to achieve a smooth and roughly circular target boundary. (b) The *data term* gives high priority to pixels on the continuation of image structures (in green) and has the effect of favouring in-pointing appendices in the direction of incoming structures. The combination of the two terms in Eq. (1) produces the desired organic balance between the two effects, where the inwards growth of image structures is enforced with moderation.

- Extract the manually selected initial front $\delta\Omega^0$.
- Repeat until done:

1a. Identify the fill front $\delta\Omega^t$. If $\Omega^t = \emptyset$, exit.
1b. Compute priorities $P(\mathbf{p}) \quad \forall \mathbf{p} \in \delta\Omega^t$.
2a. Find the patch $\Psi_{\hat{\mathbf{p}}}$ with the maximum priority, *i.e.*, $\hat{\mathbf{p}} = \arg\max_{\mathbf{p} \in \delta\Omega^t} P(\mathbf{p})$.
2b. Find the exemplar $\Psi_{\hat{\mathbf{q}}} \in \Phi$ that minimizes $d(\Psi_{\hat{\mathbf{p}}}, \Psi_{\hat{\mathbf{q}}})$.
2c. Copy image data from $\Psi_{\hat{\mathbf{q}}}$ to $\Psi_{\hat{\mathbf{p}}}$ $\forall \mathbf{p} \in \Psi_{\hat{\mathbf{p}}} \cap \Omega$.
3. Update $C(\mathbf{p}) \quad \forall \mathbf{p} \in \Psi_{\hat{\mathbf{p}}} \cap \Omega$

TABLE I
Region filling algorithm.

But, as mentioned, the pixels of the target region in the proximity of those appendices are surrounded by little confidence (most neighbouring pixels are un-filled), and therefore, the "push" due to image edges is mitigated by the confidence term. As presented in the results section, this achieves a graceful and automatic balance of effects and an organic synthesis of the target region via the mechanism of a single priority computation for all patches on the fill front. Notice that (1) only dictates the order in which filling happens. The use of image patches for the actual filling achieves texture synthesis [11].

Furthermore, since the fill order of the target region is dictated solely by the priority function $P(\mathbf{p})$, we avoid having to predefine an arbitrary fill order as done in existing patch-based approaches [11], [22]. Our fill order is function of image proper-

ties, resulting in an organic synthesis process that eliminates the risk of "broken-structure" artefacts (as in fig. 11f). Furthermore, since the gradient-based guidance tends to propagate strong edges, blocky and mis-alignment artefacts are reduced (though not completely eliminated), without a patch-cutting (quilting) step [11] or a blur-inducing blending step [22].

It must be stressed that our algorithm does not use explicit nor implicit segmentation at any stage. For instance, the gradient operator in (1) is never thresholded and real valued numbers are employed.

Implemetation details. In our implementation the contour $\delta\Omega$ of the target region is modelled as a dense list of image point locations. These points are interactively selected by the user via a simple drawing interface. Given a point $\mathbf{p} \in \delta\Omega$, the normal direction $\mathbf{n}_p$ is computed as follows: i) the positions of the "control" points of $\delta\Omega$ are filtered via a bi-dimensional Gaussian kernel and, ii) $\mathbf{n}_p$ is estimated as the unit vector orthogonal to the line through the preceding and the successive points in the list. Alternative implementation may make use of curve model fitting. The gradient $\nabla I_{\mathbf{p}}$ is computed as the maximum value of the image gradient in $\Psi_{\mathbf{p}} \cap I$. Robust filtering techniques may also be employed here. Finally, pixels are classified as belonging to the target region Ω, the source region Φ or the remainder of the image by assigning different values to their alpha component. The image alpha channel is, therefore, updated (locally) at each iteration of the filling algorithm.

IV. Results and comparisons

Here we apply our algorithm to a variety of images, ranging from purely synthetic images to full-colour photographs that include complex textures. Where possible, we make side-by-side comparisons to previously proposed methods. In other cases, we hope the reader will refer to the original source of our test images (many are taken from previous literature on inpainting and texture synthesis) and compare these results with the results of earlier work.

In all of the experiments, the patch size was set to be greater than the largest texel or the thickest structure (*e.g.*, edges) in the source region. Furthermore, unless otherwise stated the source region has been set to be $\Phi = \mathcal{I} - \Omega$. All experiments were run on a 2.5GHz Pentium IV with 1GB of RAM.

The Kanizsa triangle and the Connectivity Principle. We perform our first experiment on the well-known Kanizsa triangle [20] to show how the algorithm works on a structure-rich synthetic image.

As shown in fig. 7, our algorithm deforms the fill front $\delta\Omega$ under the action of two forces: isophote continuation (the data term, $D(\mathbf{p})$) and the "pressure" from surrounding filled pixels (the confidence term, $C(\mathbf{p})$).

The sharp linear structures of the incomplete green triangle are grown into the target region. But also, no single structural element dominates all of the others. This balance among competing isophotes is achieved through the naturally decaying confidence values (fig 10 will illustrate the large-scale artefacts which arise when this balance is missing). Figures 7e,f also show the effect of the confidence term in smoothing sharp appendices such as the vertices of the target region.

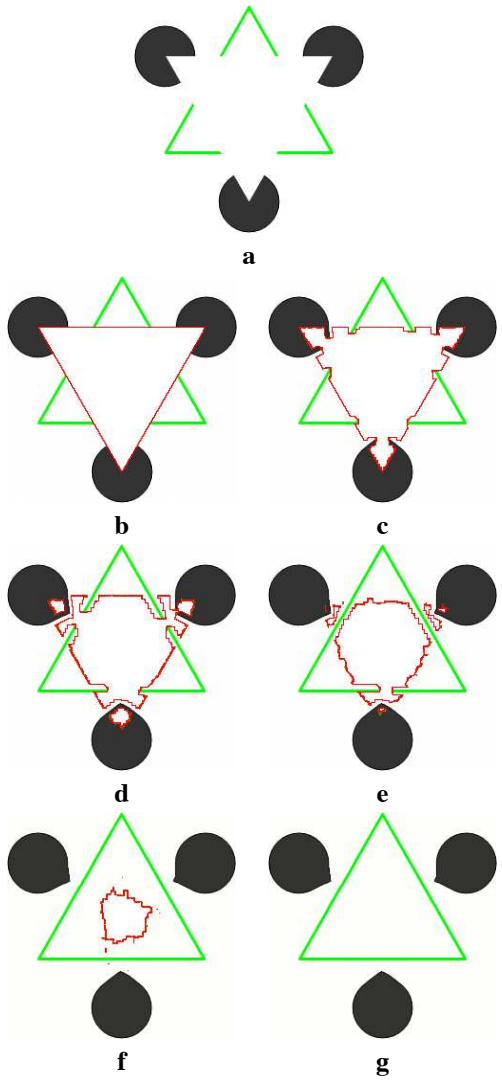

Fig. 7. **Realization of the "Connectivity Principle" on a synthetic example.** (a) Original image, the "Kanizsa triangle" with random noise added. (b) The occluding white triangle in the original image has been manually selected as the target region (24% of total image area) and marked with a red boundary. (c. . .f) Different stages of the filling process. (d) Notice that strong edges are pushed inside the target region first and that sharp appendices (*e.g.*, the vertices of the selected triangle) are rapidly smoothed. (f) When no structures hit the front $\delta\Omega$ the target region evolves in a roughly circular shape. (g) The output image where the target region has been filled, *i.e.*, the occluding triangle removed. Little imperfections are present in the curvature of the circles in the reconstructed areas, while the sides of the internal triangle have been correctly connected. The blur typical of diffusion techniques is completely avoided. See figs. 11, 13, 20 for further examples of structural continuation.

As described above, the confidence is propagated in a manner similar to the front-propagation algorithms used in inpainting. We stress, however, that unlike inpainting, it is the confidence values that are propagated along the front (and which determine fill order), not colour values themselves, which are sampled from the source region.

Finally, we note that despite the large size of the removed region, edges and lines in the filled region are as sharp as any found in the source region; *i.e.*, there is no diffusion-related blur. This is a property of exemplar-based texture synthesis.

Comparing different filling orders. Figures 8, 9 and 11 demonstrate the effect of different filling strategies.

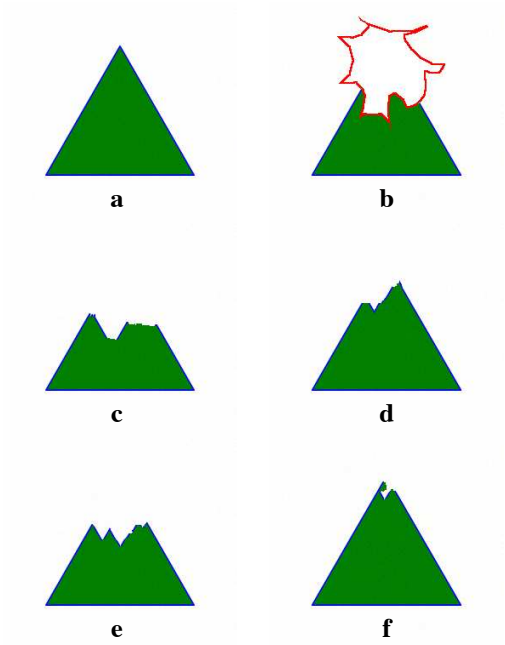

Fig. 8. **Effect of filling order on a synthetic image.** (a) The original image; (b) The target region has been selected and marked with a red boundary; (c) Filling the target region in raster-scan order; (d) Filling by concentric layers; (e) The result of applying Harrison's technique which took $2\,'\,45\,''$; (f) Filling with our algorithm which took $5\,''$. Notice that even though the triangle upper vertex is not complete our technique performs better than the others.

Figure 8f shows how our filling algorithm achieves the best structural continuation in a simple, synthetic image. Our synthesis algorithm has been compared with three other existing techniques.

Also, as stated previously, in the case only the edge term is used, then the overshoot artefact may arise, as demonstrated in fig 10.

Figure 9 further demonstrates the validity of our algorithm on an aerial photograph. The 40×40-pixel target region has been selected to straddle two different textures (fig. 9b). The remainder of the 200×200 image in fig. 9a was used as source for all the experiments in fig. 9.

With raster-scan synthesis (fig. 9c) not only does the top region (the river) grow into the bottom one (the city area), but visible seams also appear at the bottom of the target region. This problem is only partially addressed by a concentric filling (fig 9d). Similarly, in fig. 9e the sophisticated ordering proposed by Harrison [15] only moderately succeeds in preventing this phenomenon.

In all of these cases, the primary difficulty is that since the (eventual) texture boundary is the most constrained part of the target region, it should be filled first. But, unless this is explicitly addressed in determining the fill order, the texture boundary is often the last part to be filled. The algorithm proposed in this paper is designed to address this problem, and thus more naturally extends the contour between the two textures as well as the vertical grey road in the figure.

In the example in fig. 9, our algorithm synthesizes the target region in only 2 seconds. Harrison's resynthesizer [15], which is the nearest in quality, requires approximately 45 seconds.

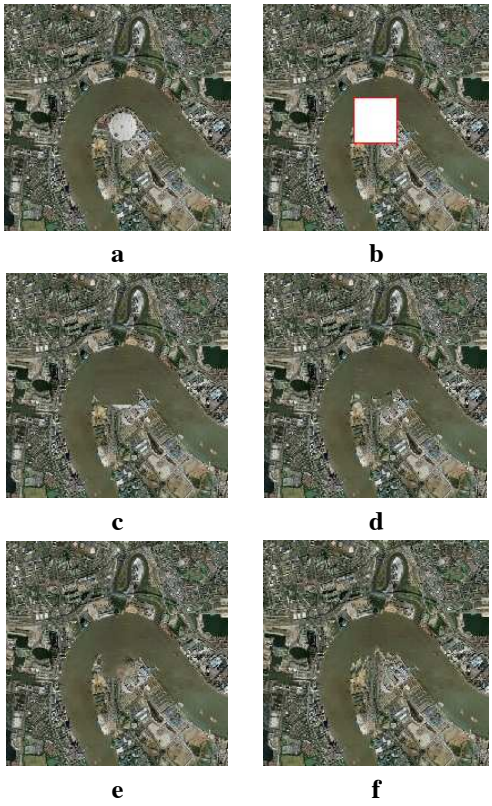

Fig. 9. **Effect of filling order on an aerial photograph.** (a) The original image, an aerial view of London. (b) The target region has been selected and marked with a red boundary; Notice that it straddles two different textures; (c) Filling with raster-scan order; (d) Filling by concentric layers; (e) The result of applying Harrison's technique (performed in $45\,''$); (f) Filling with our algorithm (performed in $2\,''$). See text for details.

Fig. 10. **The "overshoot" artefact.** The use of the data term only in the priority function may lead to undesired edge "over-shoot" artefacts. This is due to the fact that some edges may grow indiscriminately. A balance between structure and texture synthesis is highly desirable and achieved in this paper. *cf.* fig 8f.

Figure 11 shows yet another comparison between the concentric filling strategy and the proposed algorithm. In the presence of concave target regions, the "onion peel" filling may lead to visible artefacts such as unrealistically broken structures (see the pole in fig. 11f). Conversely, the presence of the data term of (1) encourages the edges of the pole to grow "first" inside the target region and thus correctly reconstruct the complete pole (fig. 11f'). This example demonstrates the robustness of the proposed algorithm with respect to the shape of the selected target region.

Figure 12 shows a visualization of the priority function related to the example in fig 11c',...,f'. Notice that due to the data term of (1) the pixels belonging to the reconstructed pole are characterized by larger (brighter) values of $P(\mathbf{p})$. Similarly, pixels on thin appendices (larger confidence) of the target region

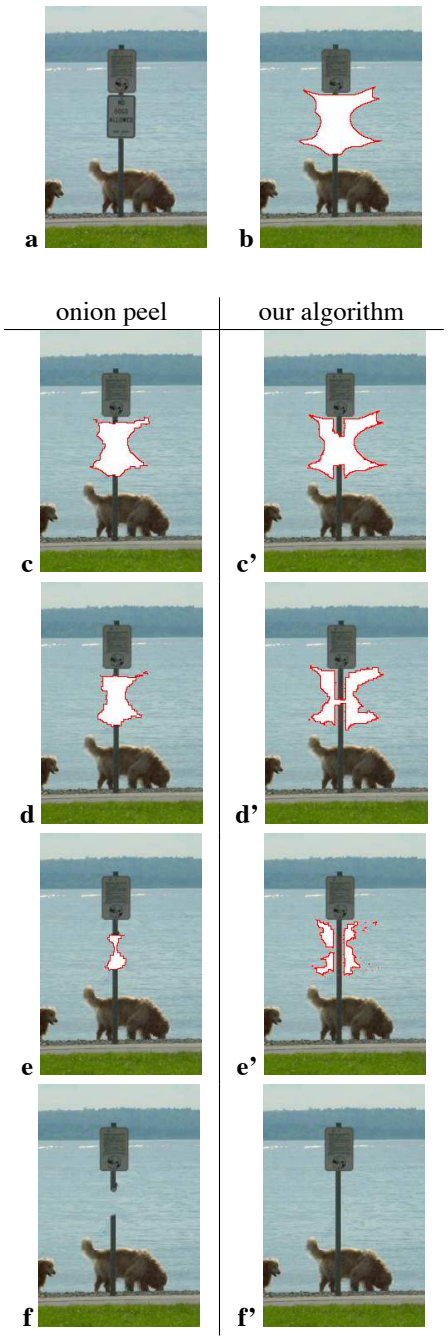

Fig. 11. **Onion peel vs. structure-guided filling.** (a) Original image. (b) The target region has been selected and marked with a red boundary. (c,d,e,f) Results of filling by concentric layers. (c',d',e',f') Results of filling with our algorithm. Thanks to the *data term* in (1) the sign pole is reconstructed correctly by our algorithm.

tend to have large priority values associated with them.

Comparisons with diffusion-based inpainting. We now turn to some examples from the inpainting literature. The first two examples show that our approach works at least as well as inpainting.

The first (fig. 13) is a synthetic image of two ellipses [4]. The occluding white torus is removed from the input image and the two dark background ellipses reconstructed via our algorithm (fig. 13b). This example was chosen by authors of the original work on inpainting to illustrate the structure propagation capabilities of their algorithm. Our results are visually identical to those obtained by inpainting (*cf.* fig.4 in [4]).

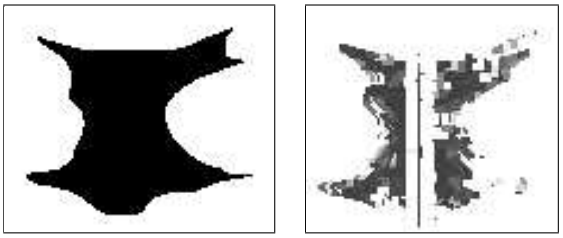

Fig. 12. **Priority function for the example in fig 11f'.** (a) The priorities associated to the target region in fig 11 are initialized as 0 inside (dark pixels) and 1 outside (bright pixels). (b) The final priorities at the end of the filling process. Notice that larger values of the priority function $P(\mathbf{p})$ are associated with pixels on the continuation of strong edges (*i.e.*, the pole) and on thin outward-pointing appendices.

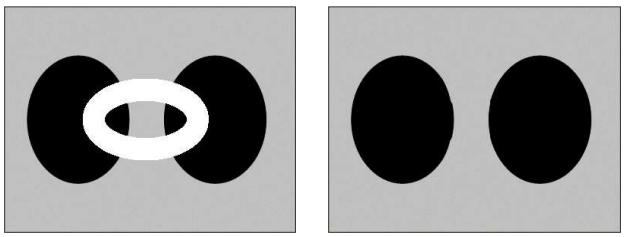

Fig. 13. **Comparison with traditional structure inpainting.** (a) Original image from [4]. The target region is the white ellipse in the centre. (b) Object removal and structure recovery via our algorithm.

We now compare results of the restoration of an hand-drawn image. In fig. 14 the aim is to remove the foreground text. Our results (fig. 14b) are mostly indistinguishable with those obtained by traditional inpainting [4]. This example demonstrates the effectiveness of both techniques in image restoration applications.

It is in real photographs with large objects to remove, however, that the real advantages of our approach become apparent. Figure 15 shows an example on a real photograph, of a bungee jumper in mid-jump (from [4], fig.8). In the original work, the thin bungee cord is removed from the image via inpainting. In order to prove the capabilities of our algorithm we removed the entire person (fig. 15e). Structures such as the shore line and the edge of the house have been automatically propagated into the target region along with plausible textures of shrubbery, water and roof tiles; and all this with no *a priori* model of anything specific to this image.

For comparison, figure 15f shows the result of filling the same target region (fig. 15b) by image inpainting[5]. Considerable blur is introduced into the target region because of inpainting's use of diffusion to propagate colour values. Moreover, high-frequency textural information is entirely absent.

Figure 16 compares our algorithm to the recent "texture and structure inpainting" technique described in [5]. The original image in fig. 16a and fig. 16b are from [5]. Figure 16c shows the result of our filling algorithm and it demonstrates that also our

[4] `www.ece.umn.edu/users/marcelo/restoration4.html`

[5] 120,000 iterations were run using the implementation in `www.bantha.org/~aj/inpainting/`

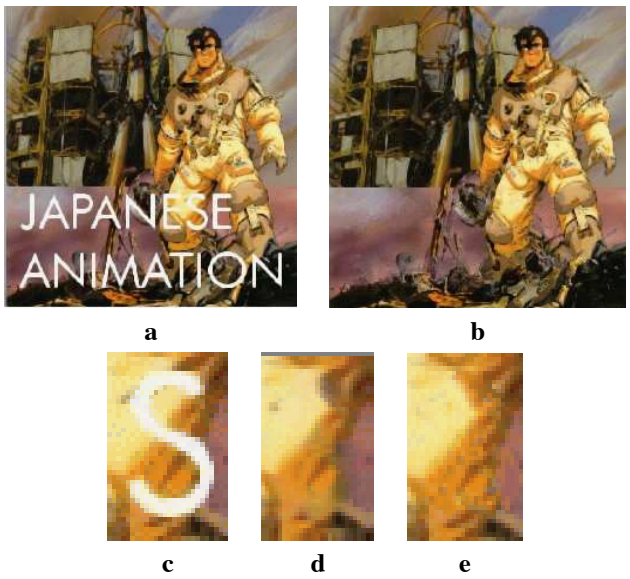

Fig. 14. **Image restoration example.** (a) Original image. The text occupies 9% of the total image area. (b) Result of text removal via our algorithm. (c) Detail of (a). (e) Result of filling the "S" via traditional image-inpainting. (d) Result of filling the "S" via our algorithm. We also achieve structure propagation.

technique accomplishes the simultaneous propagation of structure and texture inside the selected target region. Moreover, the lack of diffusion step in our method avoids blurring propagated structures (see the vertical edge in the encircled region) and makes the algorithm more computationally efficient.

Comparison with Drori *et al*. "Fragment-based Image Completion". Figure 17 shows the results of our region-filling algorithm on one of the examples used in [10]. As it can be noticed by comparing fig. 17d and the last image in fig.13 of [10], our algorithm does not introduce the edge blur that characterizes the latter figure. In fig. 17d the sharpness of the table edge is retained since no smoothing is introduced at any stage of our filling algorithm.

Comparison with Jia et al. "Image Repairing". Figure 18 compares the results of our region-filling algorithm with those obtained by Jia *et al*. in [19]. The image in fig. 18c has been obtained by the region-filling algorithm in [19], and fig. 18d shows the result of our algorithm. Notice that our algorithm succeedes in filling the target region without implicit or explicit segmentation.

Synthesizing composite textures. Fig. 19 demonstrates that our algorithm behaves well also at the boundary between two different textures, such as the ones analyzed in [26]. The original image in fig. 19a is one of the examples used in [26]. The target region selected in fig. 19c straddles two different textures. The quality of the "knitting" in the contour reconstructed via our approach (fig. 19d) is similar to the original image and to the results obtained in the original work (fig. 19b), but again, this has been accomplished without complicated texture models or a separate boundary-specific texture synthesis algorithm.

It must be stressed that in cases such as that of fig. 19c where the band around the target region does not present dominant gradient directions the filling process proceeds in a roughly uniform way, similar to the concentric-layer approach. This is achieved automatically through the priority equation (1).

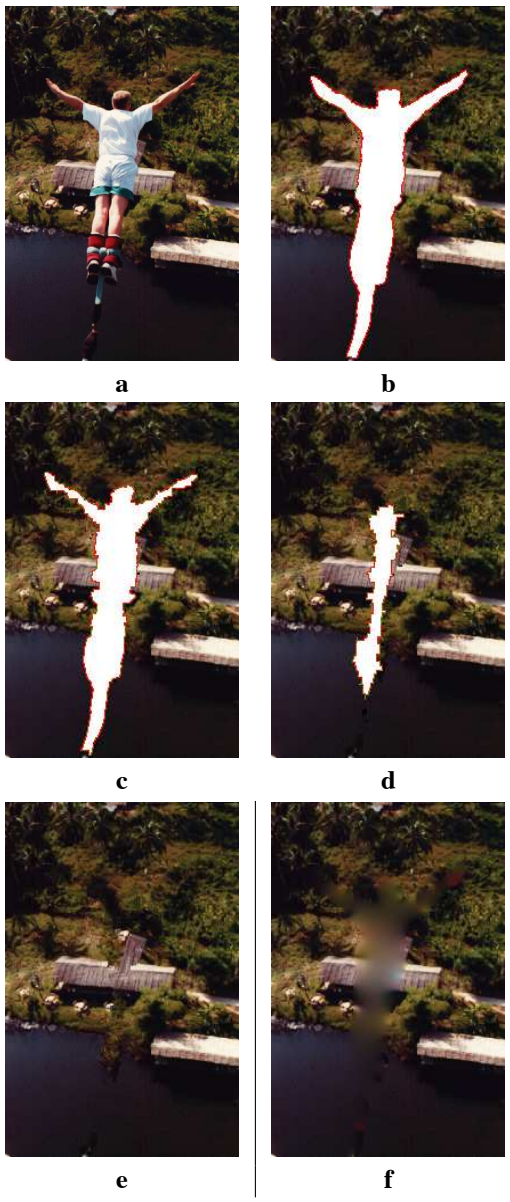

Fig. 15. **Removing large objects from photographs.** (a) Original image from [4], $205 \times 307 pix$. (b) The target region (in white with red boundary) covers 12% of the total image area. (c,d) Different stages of the filling process. Notice how the isophotes hitting the boundary of the target region are propagated inwards while thin appendices (*e.g.*, the arms) in the target region tend to disappear quickly. (e) The final image where the bungee jumper has been completely removed and the occluded region reconstructed by our automatic algorithm (performed in 18 $''$, to be compared with 10 $'$ of Harrison's resynthesizer). (f) The result of region filling by traditional image inpainting. Notice the blur introduced by the diffusion process and the complete lack of texture in the synthesized area.

Further examples on photographs. We show more examples on photographs of real scenes.

Figure 20 demonstrates, again, the advantage of the proposed approach in preventing structural artefacts. While the onion-peel approach produces a deformed horizon (fig. 20f), our algorithm reconstructs the boundary between sky and sea as a convincing straight line (fig. 20f'). During the filling process the

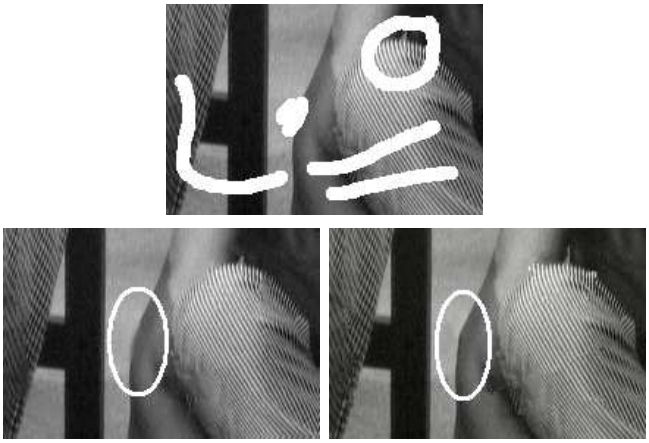

Fig. 16. **Comparison with "texture and structure inpainting" [5].** (a) Original image. The target regions are marked in white. (b) Region filling via "Simultaneous Structure and Texture Propagation". Notice the blur of the edge in the circled region. (c) The result of our algorithm. Both structure and texture have been nicely propagated inside the target region. The edge in the circled region is noticeably sharper.

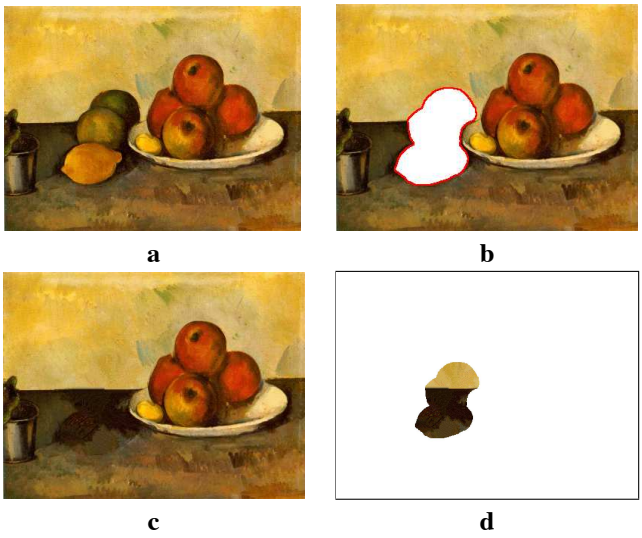

Fig. 17. **Comparison with "Fragment-Based Image Completion" [11].** (a) A photo of the oil painting "Still Life with Apples", P. Cézanne, c. 1890, The Hermitage, St. Petersburg. (b) The manually selected target region. (c) The result of our automatic region-filling algorithm. (d) The data which has been used to fill the target region. Notice the sharply reconstructed table edge, see text for details.

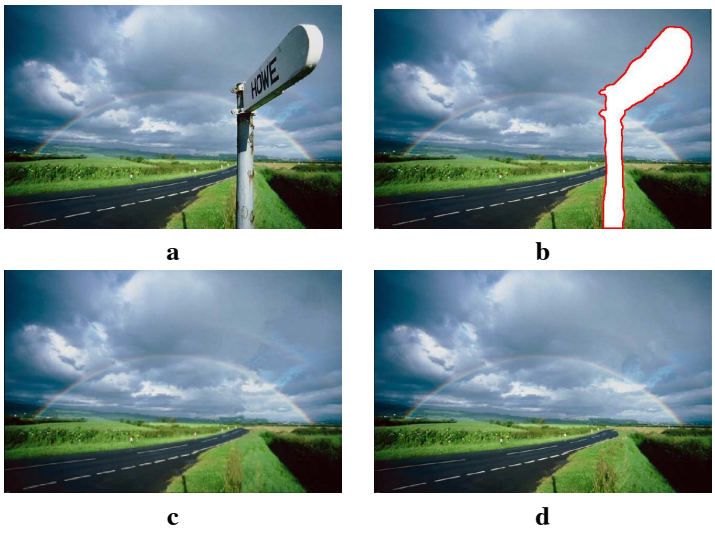

Fig. 18. **Comparison with Jia et al. "Image Repairing" [20].** (a) `Moor`, original input image. (b) The manually selected target region. (c) The resulting region-filling achieved by *Jia et al.* . (d) The result of our region-filling algorithm. The missing portion of rainbow is reconstructed convincingly. Figures (c) and (d) are of comparable quality, but our algorithm avoids the image segmentation step with considerable increase in speed.

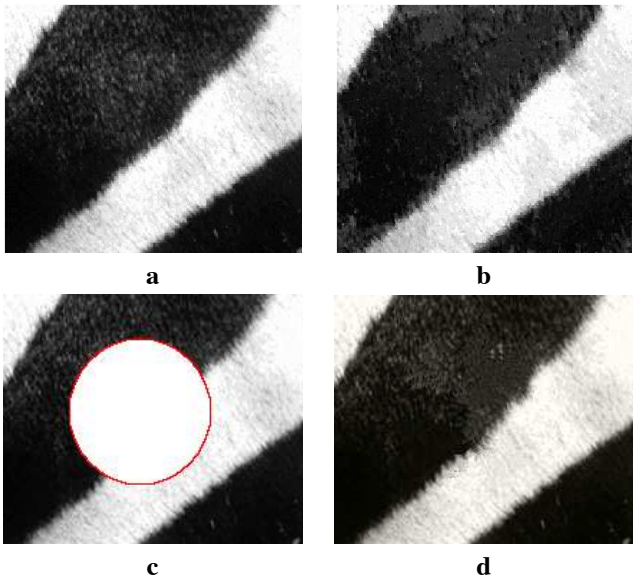

Fig. 19. **Comparison with "Parallel Composite Texture Synthesis" [27].** (a) Original image, the fur of a zebra. (b) The result of the synthesis algorithm described in "Parallel Composite Texture Synthesis". (c) Original image with the target region marked with a red boundary (22% of total image size). (d) The target region has been filled via our algorithm. The "knitting" effect along the boundary between the two textures is correctly reproduced also by our technique.

topological changes of the target region are handled effortlessly.

In fig. 21, the foreground person has been manually selected and the corresponding region filled in automatically. The synthesized region in the output image convincingly mimics the complex background texture with no prominent artefacts (fig. 21f).

Finally, figs 22... 27 present a gallery of further examples of object removal and region filling from real photographs. Those results demonstrate the power and versatility of our algorithm.

V. Conclusion and Future Work

This paper has presented a novel algorithm for removing *large* objects from digital photographs. The result is an image in which the selected object has been replaced by a visually plausible background that mimics the appearance of the source region.

Our approach employs an exemplar-based texture synthesis technique modulated by a unified scheme for determining the *fill order* of the target region. Pixels maintain a confidence value, which together with image isophotes, influence their fill priority.

The technique is capable of propagating both linear structure and two-dimensional texture into the target region with a single, simple algorithm. Comparative experiments show that a simple selection of the fill order is necessary *and* sufficient to handle

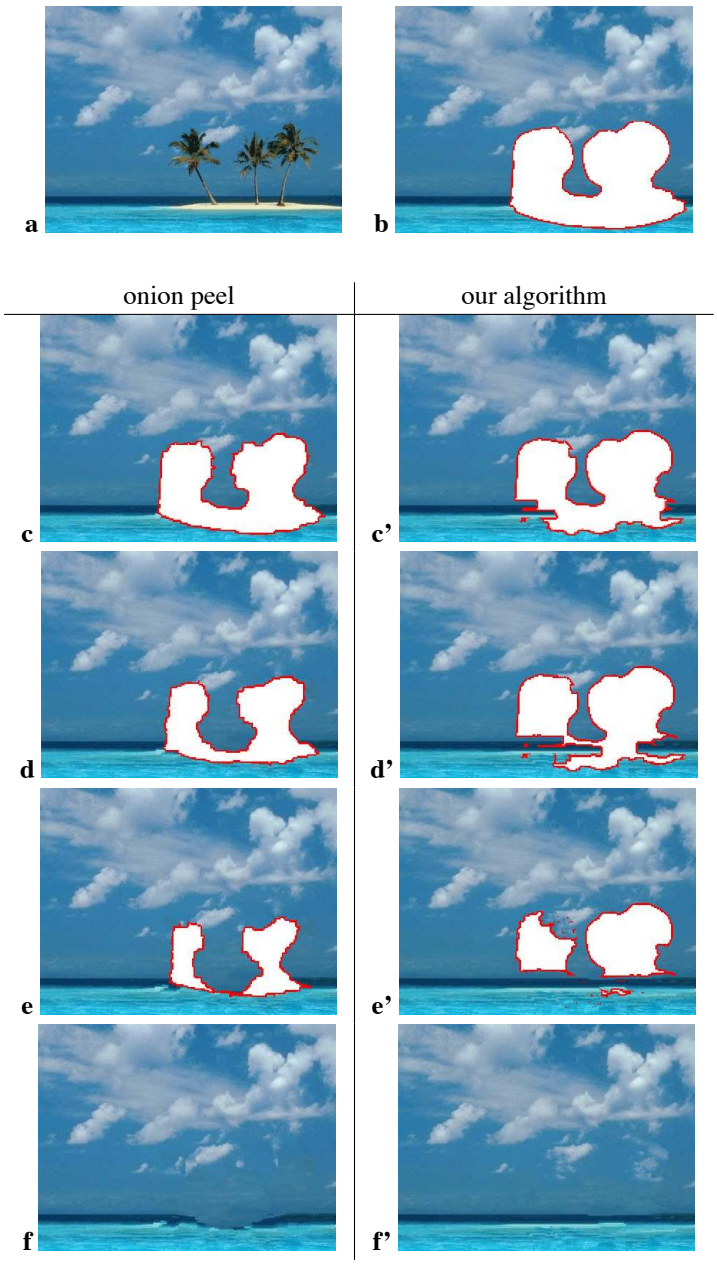

Fig. 20. **Concentric-layer filling vs. the proposed guided filling algorithm.** (a) Original image. (b) The manually selected target region (20% of the total image area) has been marked in white with a red boundary. (c,d,e,f) Intermediate stages in the concentric-layer filling. The deformation of the horizon is caused by the fact that in the concentric-layer filling sky and sea grow inwards at uniform speed. Thus, the reconstructed sky-sea boundary tends to follow the *skeleton* of the selected target region. (c',d',e',f') Intermediate stages in the filling by the proposed algorithm, where the horizon is correctly reconstructed as a straight line.

this task.

Our method performs at least as well as previous techniques designed for the restoration of *small* scratches, and, in instances in which *larger* objects are removed, it dramatically outperforms earlier work in terms of both perceptual quality and computational efficiency.

Moreover, robustness towards changes in shape and topology of the target region has been demonstrated, together with other advantageous properties such as: (i) preservation of edge sharp-

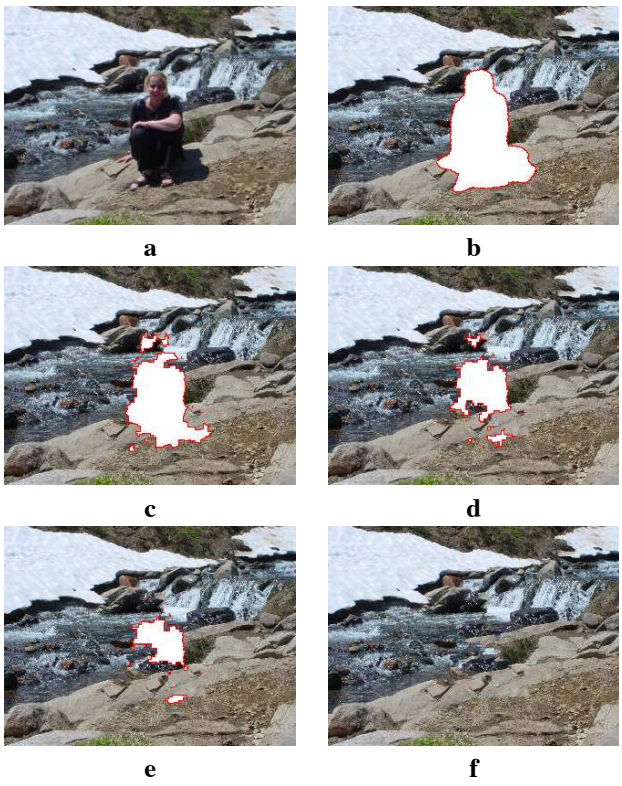

Fig. 21. **Removing large objects from photographs.** (a) Original image. (b) The target region (10% of the total image area) has been blanked out. (c. . .e) Intermediate stages of the filling process. (f) The target region has been completely filled and the selected object removed. The source region has been automatically selected as a band around the target region. The edges of the stones have been nicely propagated inside the target region together with the water texture.

Fig. 22. **Removing an object on a highly textured background.** (a) Original photograph. (b) One of the two people has been removed. This demonstrates that our algorithm works correctly also for the (simpler) case of "pure" texture.

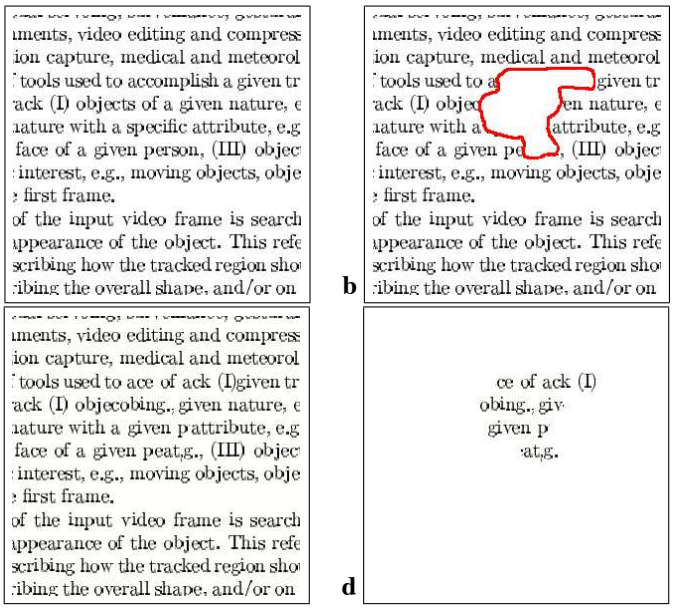

Fig. 23. **Region-filling on an image of a text.** (a) Original photo of typewritten text, a favourite example of texture synthesis researchers. (b) A portion of the image (marked with a red boundary) has been removed. (c) The result of our filling algorithm. (d) As in (c) with just the text synthesized in the target region highlighted. Even though the generated text does not make much sense it still looks plausible. This example further demonstrates the correct behaviour of our algorithm in the case of pure texture synthesis.

Fig. 24. **Removing several objects from a photograph.** (a) Original image, a photograph from Ghana. Courtesy of P. Anandan. (b,c) The crowd of people and other objects are gradually removed by our algorithm. The source regions have been selected as dilated bands around the target regions. Background texture and structure have seamlessly replaced the original characters.

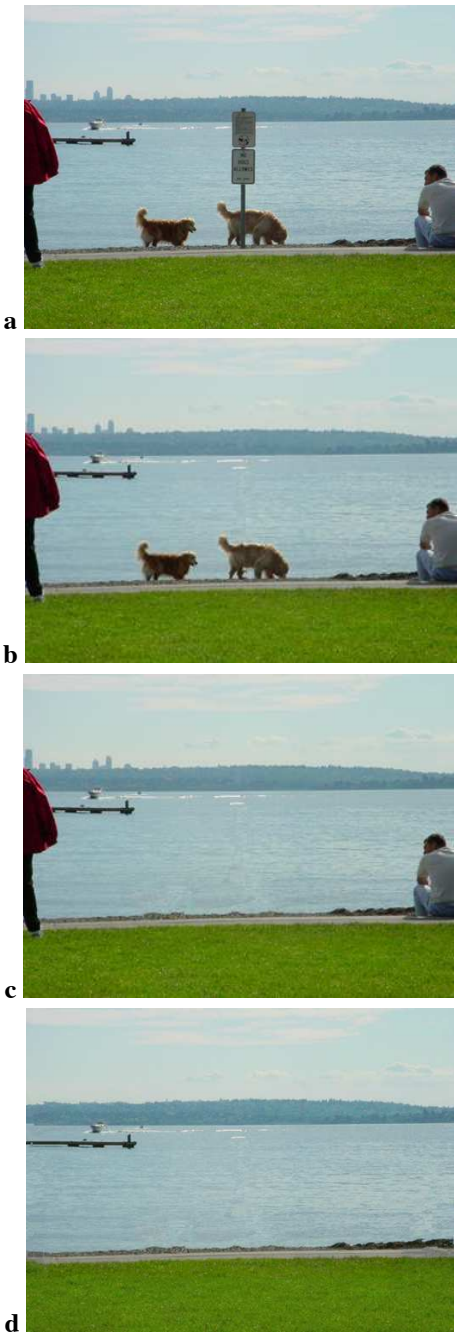

Fig. 25. **Removing multiple objects from photographs.** (a) Original photograph of Kirkland (WA). (b,c,d) Several objects are sequentially removed. Notice how well the shore line and other structures have been reconstructed.

ness, (ii) no dependency on image segmentation and (iii) balanced region filling to avoid over-shooting artefacts.

Also, patch-based filling helps achieve: (i) speed efficiency, (ii) accuracy in the synthesis of texture (less garbage growing), and finally (iii) accurate propagation of linear structures.

Limitations of our technique are: (i) the synthesis of regions for which similar patches do not exist does not produce reasonable results (a problem common to [10], [19]); (ii) the algorithm is not designed to handle curved structures, (iii) finally, like in [10], [19], our algorithm does not handle depth ambiguities (*i.e.*, what is in front of what in the occluded area?).

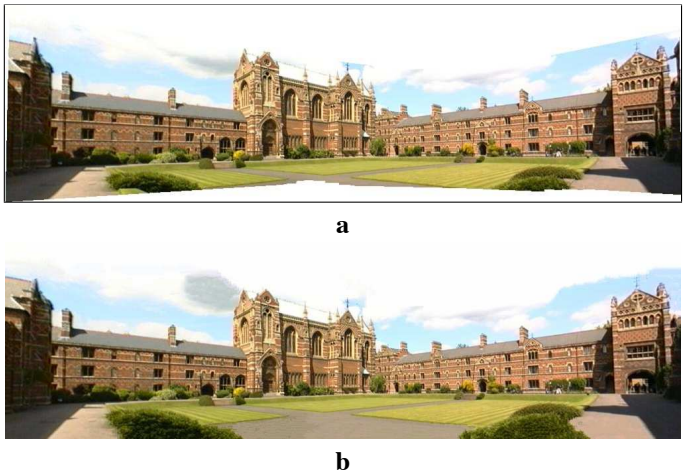

Fig. 26. **Completing panoramas.** (a) A panorama of Keble College in Oxford. Courtesy of D. Capel and A. Zisserman [7]. (b) The "bow-tie" effect which characterizes image stitching has been removed here by automatic region in-filling.

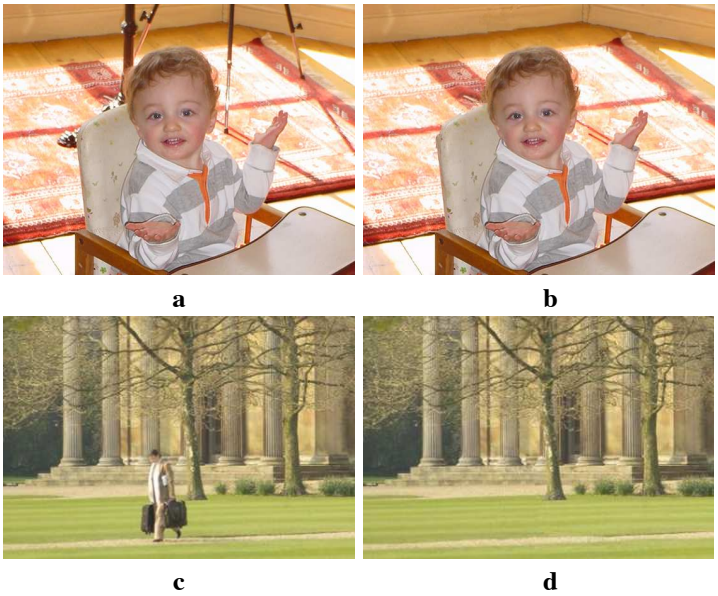

Fig. 27. **Final examples of object removal from photographs.** (a,c) Original images. (b,d) After object removal. Objects and people are removed by realistic edge and texture synthesis in the selected target regions.

Currently, we are investigating the possibility of constructing ground-truth data and designing evaluation tests that would allow us to quantify the performance of each algorithm. This turns out to be a non-trivial task. Furthermore we are ivestigating extensions of the current algorithm to handle accurate propagation of curved structures in still photographs as well as removing objects from video, which promise to impose an entirely new set of challenges.

Acknowledgements. The authors would like to thank M. Gangnet, A. Blake, P. Anandan and R. Bornard for inspiring discussions; and G. Sapiro, M. Bertalmio, D. Capel, A. Zisserman, L. van Gool and A. Zalesny for making some of their images available.

REFERENCES

[1] M. Ashikhmin. Synthesizing natural textures. In *Proc. ACM Symposium on Interactive 3D Graphics*, pages 217–226, Research Triangle Park, NC, March 2001.

[2] C. Ballester, V. Caselles, J. Verdera, M. Bertalmio, and G. Sapiro. A variational model for filling-in gray level and color images. In *Proc. Int. Conf. Computer Vision*, pages I: 10–16, Vancouver, Canada, June 2001.

[3] M. Bertalmio, A.L. Bertozzi, and G. Sapiro. Navier-stokes, fluid dynamics, and image and video inpainting. In *Proc. Conf. Comp. Vision Pattern Rec.*, pages I:355–362, Hawai, December 2001.

[4] M. Bertalmio, G. Sapiro, V. Caselles, and C. Ballester. Image inpainting. In *Proc. ACM Conf. Comp. Graphics (SIGGRAPH)*, pages 417–424, New Orleans, LU, July 2000. `http://mountains.ece.umn.edu/~guille/inpainting.htm`.

[5] M. Bertalmio, L. Vese, G. Sapiro, and S. Osher. Simultaneous structure and texture image inpainting. In *Proc. Conf. Comp. Vision Pattern Rec.*, Madison, WI, 2003. `http://mountains.ece.umn.edu/~guille/inpainting.htm`.

[6] R. Bornard, E. Lecan, L. Laborelli, and J-H. Chenot. Missing data correction in still images and image sequences. In *ACM Multimedia*, France, December 2002.

[7] T. F. Chan and J. Shen. Non-texture inpainting by curvature-driven diffusions (CDD). *J. Visual Comm. Image Rep.*, 4(12):436–449, 2001.

[8] A. Criminisi, P. Perez, and K. Toyama. Object removal by exemplar-based inpainting. In *Proc. Conf. Comp. Vision Pattern Rec.*, Madison, WI, Jun 2003.

[9] J.S. de Bonet. Multiresolution sampling procedure for analysis and synthesis of texture images. In *Proc. ACM Conf. Comp. Graphics (SIGGRAPH)*, volume 31, pages 361–368, 1997.

[10] I. Drori, D. Cohen-Or, and H. Yeshurun. Fragment-based image completion. In *ACM Trans. on Graphics (SIGGRAPH 2003 issue), 22(3)*, volume 22, pages 303–312, San Diego, US, 2003.

[11] A. Efros and W.T. Freeman. Image quilting for texture synthesis and transfer. In *Proc. ACM Conf. Comp. Graphics (SIGGRAPH)*, pages 341–346, Eugene Fiume, August 2001.

[12] A. Efros and T. Leung. Texture synthesis by non-parametric sampling. In *Proc. Int. Conf. Computer Vision*, pages 1033–1038, Kerkyra, Greece, September 1999.

[13] W.T. Freeman, E.C. Pasztor, and O.T. Carmichael. Learning low-level vision. *Int. J. Computer Vision*, 40(1):25–47, 2000.

[14] D. Garber. *Computational Models for Texture Analysis and Texture Synthesis*. PhD thesis, University of Southern California, USA, 1981.

[15] P. Harrison. A non-hierarchical procedure for re-synthesis of complex texture. In *Proc. Int. Conf. Central Europe Comp. Graphics, Visua. and Comp. Vision*, Plzen, Czech Republic, February 2001.

[16] D.J. Heeger and J.R. Bergen. Pyramid-based texture analysis/synthesis. In *Proc. ACM Conf. Comp. Graphics (SIGGRAPH)*, volume 29, pages 229–233, Los Angeles, CA, 1995.

[17] A. Hertzmann, C. Jacobs, N. Oliver, B. Curless, and D. Salesin. Image analogies. In *Proc. ACM Conf. Comp. Graphics (SIGGRAPH)*, Eugene Fiume, August 2001.

[18] H. Igehy and L. Pereira. Image replacement through texture synthesis. In *Proc. Int. Conf. Image Processing*, pages III:186–190, 1997.

[19] J. Jia and C.-K. Tang. Image repairing: Robust image synthesis by adaptive nd tensor voting. In *Proc. Conf. Comp. Vision Pattern Rec.*, Madison, WI, 2003.

[20] G. Kanizsa. *Organization in Vision*. Praeger, New York, 1979.

[21] J. M. Kasson and W. Plouffe. An analysis of selected computer interchange color spaces. In *ACM Transactions on Graphics*, volume 11, pages 373–405, October 1992.

[22] L. Liang, C. Liu, Y.-Q. Xu, B. Guo, and H.-Y. Shum. Real-time texture synthesis by patch-based sampling. *ACM Transactions on Graphics*, 2001.

[23] S Masnou and J.-M. Morel. Level lines based disocclusion. In *Int. Conf. Image Processing*, Chicago, 1998.

[24] S. Rane, G. Sapiro, and M. Bertalmio. Structure and texture filling-in of missing image blocks in wireless transmission and compression applications. In *IEEE. Trans. Image Processing*, 2002. to appear.

[25] L.-W. Wey and M. Levoy. Fast texture synthesis using tree-structured vector quantization. In *Proc. ACM Conf. Comp. Graphics (SIGGRAPH)*, 2000.

[26] A. Zalesny, V. Ferrari, G. Caenen, and L. van Gool. Parallel composite texture synthesis. In *Texture 2002 workshop - ECCV*, Copenhagen, Denmark, June 2002.